1970-12

Elliptical Evaporation Tanks with Vertical Base and Cover Plates

Koehler, W.F.; Ashley, E.J.

worst possible choice as far as aberration is concerned. The stepped solid line across the graph indicates the refractive index values for which a flat plate will produce less (spherical) aberration than a flat plate with refractive index of 1.2. Thus, for an optical system with a 30° half-angle, the longitudinal spherical aberration due to a flat plate is worst if the plate's refractive index is about 1.6. In this case, the longitudinal (spherical) aberration will be 5.5% of the plate's thickness. Replacing this plate with an equally thick plate whose refractive index is 3.2 or greater will reduce the aberration to as little or less than it would be if a plate or refractive index of 1.2 could be obtained.

To understand why a very high refractive index plate will produce less aberration than a plate with moderate refractive index, it is merely necessary to consider the fact that for a very high refractive index plate, incident rays will pass through very close to normal. Because of this, all rays tend to be nearly parallel while in the plate. The net effect is that while in the plate, the rays neither come any closer together in the sense of focusing, nor do they develop any aberration. The rays exit the plate almost exactly the way they entered, in spacing and orientation. The main effect is displacement of the focal plane by nearly the full thickness of the plate. In a lower refractive index plate, the rays do tend to converge, but because of violation of the sine condition, aberration is introduced. (For unity refractive index there is, of course, no violation of the sine condition.)

Elliptical Evaporation Tanks with Vertical Base and Cover Plates

W. F. Koehler and E. J. Ashley

W. F. Koehler is with the Naval Postgraduate School, Monterey, California 93940; E. J. Ashley is with the Michelson Laboratory, China Lake, California 93555.

Received 28 August 1970.

It seems worthwhile to report on a unique, economical, and effective design of evaporation tanks. Such tanks have been in continuous use for fifteen years at Michelson Laboratory, producing research quality evaporated films. Briefly, each tank consists of a 83.8 cm × 50.8 cm × 1.9 cm vertical stainless steel (316) base plate and a 83.8 cm × 50.8 cm × 2.5 cm vertical Pittsburgh Duplate two-ply laminated glass cover plate (four-ply laminates are unsatisfactory), separated by an 20.3-cm wide stainless steel elliptical hoop having a 76.2-cm major axis and an 45.7-cm minor axis, as shown in Fig. 1. The steel fins welded on the sides provide additional support to the ellipse. The base and cover plate seals are provided by L-shaped neoprene gaskets which are commercially available for 61.0-cm bell jars. When considerable heating of the substrates is required, Viton L-shaped gaskets are substituted for the neoprene gaskets. Figure 2 shows two tanks separated by approximately 71.1 cm to provide the necessary space for a forepump, diffusion pump, valves, and piping to evacuate either tank. A single set of instruments and power supplies is used for both tanks of such a dual arrangement, which provides for additional economies of construction and maintenance. Such a dual arrangement requires a minimum laboratory space of 50.8 cm × 121.9 cm × 152.4 cm and provides for routine evaporations at pressures in the vicinity of 10^{-7}–10^{-8} Torr.

The large ratio of base plate area to evacuated volume in the elliptical evaporation tank provides the following advantages over conventional glass bell jars: (1) shorter pumping time, (2) larger source-to-substrate distance, (3) larger internal area for the attachment of measuring and control devices, (4) larger window area for observation during an evaporation, and (5) greater flexibility of internal arrangement of component parts for general experimental work. When a 45.7-cm coating distance is used with a rotating sample holder, variations in the thickness of evaporated films are minimal. For example, a 2000-Å-thick evaporated aluminum film had an average thickness variation of ± 16 Å over 1 cm distance on the sample, with a maximum spread in readings of ±28 Å. Two samples mounted adjacent to each other on the turntable had average thicknesses which differed by 15 Å from each other. These measurements were made interferometrically using fringes of equal chromatic order[1]; the measuring sensitivity was about ±6 Å.

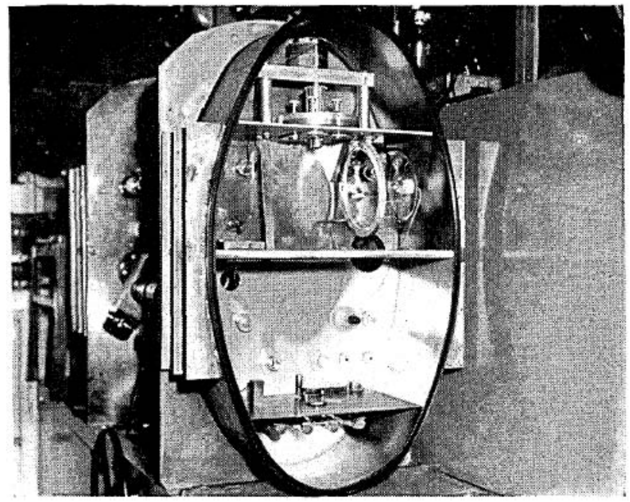

Fig. 1. Front view of elliptical evaporation tank.

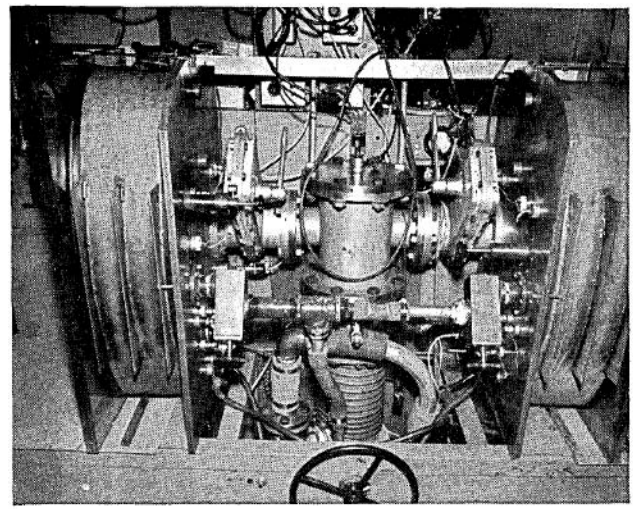

Fig. 2. Side view of elliptical evaporation tanks and associated pumping system.

The vertical arrangement of the base and cover plates provides the following advantages: (1) ease of cleaning internal surfaces of the evaporation tank; (2) ease of loading the tank including substrates, measuring instruments, control devices, evaporation sources, and evaporation materials; (3) ease of making external base plate attachments; and (4) ease of both internal and external maintenance of the entire system. The minimum time required to tear down and completely clean one tank, replace all feedthroughs and gaskets is about 2 hr. Pumpdown time is approximately 30 min to a pressure of 10^{-6} Torr; the pressure will drop to about 4×10^{-8} Torr in 4–6 h using liquid nitrogen, and evaporations can be done in the low 10^{-7} Torr or high 10^{-8} Torr range. Another significant advantage of such a system is cost. Six complete tanks were made for less than the cost of one commercially available system.

A wide variety of materials have been evaporated in these tanks, including films used in studies of optical and solid state properties[2–15] as well as films provided as a service. Silver, gold, aluminum, germanium, copper, selenium, tellurium, indium, magnesium fluoride, calcium fluoride, lead fluoride, lead chloride, and black gold have been evaporated using boats or filaments. With an electron beam gun, additional materials such as silicon, quartz, and aluminum oxide have been evaporated.

In summary, this design of evaporation system is convenient, efficient, simple, and cheap. It is easily adapted to various laboratory requirements and has proved its worth as a flexible and useful design.

The authors wish to thank L. Hahn for the nonroutine fabrication, grinding, and machining of the elliptical hoops and the vertical base plates. The many helpful discussions and measurements contributed by H. E. Bennett and J. M. Bennett are gratefully acknowledged.

References

1. H. E. Bennett and J. M. Bennett, in *Physics of Thin Films* (Academic, New York, 1967), Vol. 4, pp. 31–37.
2. W. F. Koehler, J. Opt. Soc. Amer. **48,** 55 (1958).
3. W. F. Koehler, F. K. Odencrantz, and W. C. White, J. Opt. Soc. Amer. **49,** 109 (1959).
4. H. E. Bennett, J. M. Bennett, and E. J. Ashley, J. Opt. Soc. Amer. **52,** 1245 (1962).
5. H. E. Bennett, J. Opt. Soc. Amer. **53,** 1389 (1963).
6. T. M. Donovan, E. J. Ashley, and H. E. Bennett, J. Opt. Soc. Amer. **53,** 1403 (1963).
7. J. M. Bennett, J. Opt. Soc. Amer. **54,** 612 (1964).
8. T. M. Donovan and E. J. Ashley, J. Opt. Soc. Amer. **54,** 1141 (1964).
9. J. M. Bennett, E. J. Ashley, and H. E. Bennett, Appl. Opt. **4,** 961 (1965).
10. D. K. Burge, J. M. Bennett, R. L. Peck, and H. E. Bennett, Surface Sci. **16,** 303 (1969).
11. H. E. Bennett, R. L. Peck, D. K. Burge, and J. M. Bennett, J. Appl. Phys. **40,** 3351 (1969).
12. J. L. Stanford and H. E. Bennett, Appl. Opt. **8,** 2556 (1969).
13. J. M. Bennett, J. L. Stanford, and E. J. Ashley, J. Opt. Soc. Amer. **60,** 224 (1970).
14. W. E. Spicer and T. M. Donovan, J. Non-Cryst. Solids **2,** 66 (1970).
15. T. M. Donovan, W. E. Spicer, J. M. Bennett, and E. J. Ashley, Phys. Rev. B **2,** 397 (1970).

Moiré Topography for the Measurement of Film Flatness

T. Tsuruta, Y. Itoh, and S. Anzai

Nippon Kogaku K.K., Nishi-Oi, Shinagawaku, Tokyo, Japan.
Received 6 July 1970.

Production of contour lines of height variations by use of moiré fringes has long been a well-known method of measuring mechanical deformation.[1] Recently, the advent of lasers and holography has stimulated the diffusion of this technique into a wider area of optical metrology, and a number of applications have been published.[2–6] In this article, we describe a method developed for the flatness measurement of film incorporated into a 35-mm miniature camera. In order to ensure image recording of good definition, the film must be as flat as possible, the allowance being around $\pm 0.02F$ mm, where F is an F number of the lens to be incorporated. Until now, a microscope was employed to determine the height variations of the film at several points over the aperture area of the frame. By the moiré method, on the contrary, contour lines are obtained over the whole area of the frame by a single observation. This may greatly help to estimate factors which have grave influence upon the flatness of the film.

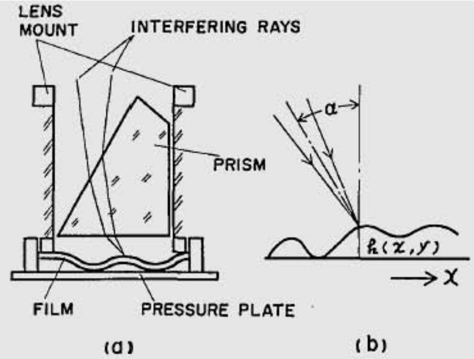

Fig. 1. (a) Experimental arrangement for projecting closely spaced equidistant straight fringes from the oblique direction upon a film incorporated into a camera. (b) Geometry illustrating the projection of fringes.

In the conventional moiré contouring method,[5] a system of two-beam interference fringes of close spacing is projected from the oblique direction upon the surface to be measured. In our experiment, however, the film is situated at the bottom of the camera and the lens mount prevents rays from falling upon the film as shown in Fig. 1(a). This difficulty was overcome by placing a prism immediately in front of the film and by introducing two plane waves from a He–Ne laser at some angle to each other with their mean angle of incidence α to the vertical. This angle can be calculated from the apex angle 60° and the refractive index 1.52 of the prism. A photographic plate of Kodak 649F is placed and exposed in position instead of the film as a reference plane and records nonlocalized equidistant straight fringes. The intensity distribution $I_0(x,y)$ is given, apart from a constant factor, by

$$I_0(x,y) = 1 + \cos(2\pi px + \Delta_0), \tag{1}$$

where x is taken perpendicular to the projected fringes, the y axis is in the plane of the plate at right angles to the x axis, p is the spatial frequency of the fringes, and Δ_0 is the phase at the origin. Keeping the whole apparatus, especially the camera, stationary, we load a roll of film into the camera and record the same fringes as recorded in the plate. The projected fringes deform owing to the lack of flatness of the film, and the intensity distribution $I_1(x,y)$ is given by

$$I_1(x,y) = 1 + \cos\{2\pi p[x + \tan\alpha \cdot h(x,y)] + \Delta_1\}, \tag{2}$$

where $h(x,y)$ is the height variation of the film, α is the mean angle of incidence of the waves, and Δ_1 is the phase at the origin. The negative of the film whose transparencies are supposed proportional to Eq. (2) is placed in contact between thin sheets of glass. The thinner sheet of 0.17 mm thickness for use in microscopy covers the back side of the film and is located as near as possible to the emulsion of the plate with the images of the frame exactly coinciding to each other. The one negative is made adjustable of declination as shown in Fig. 2. The two negatives are